American Mineralogist, Volume 74, pages 1130–1141, 1989

Distinct defect centers at oxygen positions in albite

IVAN PETROV, ANDREAS AGEL, S. S. HAFNER
Institute of Mineralogy, University of Marburg, Hans-Meerwein-Strasse, 3550 Marburg, West Germany

ABSTRACT

Metastable electron-hole centers in single crystals of Amelia albite were studied using electron paramagnetic resonance at 9.2 GHz between 5 and 260 K. Six distinct O^{1-} centers were identified as four $O^{1-}/2^{27}Al$ centers, one $O^{1-}/^{27}Al \times 2^{23}Na$ center, and one $O^{1-}/[Si,M^{2+}]$ center. Values of their **g** and **A** tensors and limits of thermal stabilities were determined.

The four $O^{1-}/2^{27}Al$ centers could be assigned to $Al_{T1(O)}$–$O_{C(O)}$–$Al_{T2(m)}$, $Al_{T1(O)}$–$O_{D(O)}$–$Al_{T2(m)}$, $Al_{T2(O)}$–$O_{C(m)}$–$Al_{T1(m)}$, and $Al_{T2(O)}$–$O_{D(m)}$–$Al_{T1(m)}$ bridges (violations of the rule of Loewenstein) and are designated as c_O, d_O, c_m, and d_m, respectively. Their total concentration was estimated to be 2×10^{-4} to 3×10^{-4} per formula unit $NaAlSi_3O_8$. Their spectra could be observed between 5 and 220 K, the maximum intensities being near $T_m = 60$ K. They were destroyed after heating at 523 K for 3 h. The calculated density of the O^{1-} ($2p^5$) unpaired electron at the tetrahedral Al position is about 0.006 e.

The $O^{1-}/^{27}Al \times 2^{23}Na$ center could be assigned to a $Si_{T1(O)}$–O_{A1}–$Al_{T1(m)}$ bridge and is designated as a_1'. Its estimated concentration is at least 1×10^{-4} per formula unit. The spectrum could be observed between 20 and 120 K, $T_m \approx 110$ K. It was destroyed after heating at 493 K for 3 h. The O^{1-} ($2p^5$) unpaired electron density at the Al position is about the same as that of the $O^{1-}/2^{27}Al$ center and 0.002 e at the two adjacent Na positions. The covalent participation in the Al–O bond is at least 50% greater than that of Al substituted for Si in quartz.

The $O^{1-}/[Si,M^{2+}]$ center could be assigned to O^{1-} at the D(m) position that links T2(O) with T1(m) and is designated as h_m. Its estimated concentration is at least 1×10^{-4} per formula unit. Its line could be observed between 10 and 260 K, $T_m \approx 115$ K. It was destroyed after heating at 623 K for 3 h.

After destruction by heating, all centers could be reactivated by X-rays.

INTRODUCTION

In general, natural alkali feldspars $(K,Na)_kAl_lSi_mO_n$ possess quite stoichiometric chemical compositions, the ratio k:l:m:n being close to 1:1:3:8. Although precise analytical data on vacancies at the atomic positions are not available, the deviations of k, l, m, and n from their ideal values are probably less than 10^{-3}. However, the number of vacancies per formula unit will certainly depend on P, T, P_{O_2}, P_{H_2O}, etc., although quantitative thermodynamic relationships are not available for alkali feldspars. Vacancies are important when the kinetics of intracrystalline atomic exchange reactions are considered, e.g., the exchange of Al and Si among the tetrahedral sites in order-disorder processes.

In this paper, new data are reported on metastable electron holes at oxygen positions, i.e., the existence of metastable O^{1-} ions, that are paramagnetic and, therefore, may be studied using electron paramagnetic resonance (EPR). Such holes are expected to be associated with structural defects in their local environment that give rise to a deficiency of positive charge, in order to attain charge compensation. Defects of this type may be vacancies or foreign cations with less positive charge than the structural ion they substitute for. The most likely point defects compensated by O^{1-} in feldspars may be a vacancy at the position of K or Na or "forbidden" Al–O–Al bridges, i.e., violations of the principle of Loewenstein (1954). In a Ca-free, completely ordered domain of low albite, formation of Al–O–Al bridges requires Al:Si ratios to be $>1:3$ and location of an Al ion at a position occupied nominally by Si.

Electron holes at oxygen positions in alkali feldspars may be produced by natural gamma radiation from the rock or artificial radiation (e.g., by X-rays). The EPR spectrum of O^{1-} consists in principle of one resonance line with $g \geq 2$, which can be observed in feldspars generally at temperatures well below 295 K. The hole center can be reversibly destroyed by heating the crystal to temperatures of 473–673 K for a few hours and reactivated by subsequent irradiation. The EPR line may be split by interaction with nuclear magnetic moments ($I \neq 0$) of cationic isotopes at adjacent positions, e.g., ^{27}Al ($I = 5/2$) and/or ^{23}Na ($I = 3/2$), yielding superhyperfine structure (SHFS).

In this work, SHF interaction of the electronic spins of O^{1-} with nuclear magnetic moments of adjacent cations was used primarily for crystallographic identification of

0003–004X/89/0910–1130$02.00

O^{1-} positions and defects in their local environment. This was achieved by determination of the characteristic **g** tensors, number of lines in the SHFS spectra, and SHF coupling constants A.

O^{1-} centers with adjacent nuclei Y, Z, etc. ($I \neq 0$) and cations M ($I = 0$) will be designated as

$$O^{1-} \Big/ \sum_{i=1}^{m} Y_i \times \sum_{j=1}^{n} Z_j \times \cdots$$

and

$$O^{1-} \Big/ \left[\sum_{i=1}^{n} M_i \right],$$

respectively. In this paper Y = ^{27}Al, Z = ^{23}Na, M_i = unidentified cation, e.g., Si^{4+}, Mg^{2+}.

EPR CENTERS DUE TO O^{1-} AND OXYGEN VACANCIES IN IRRADIATED ALKALI FELDSPAR

In the past two decades, several O^{1-} defect centers in crystals of alkali feldspar have been described, although identification has been controversial in some cases, mainly because of incomplete EPR data. Nine different types of EPR hole and electron centers due to O^{1-} or oxygen vacancies are listed below:

1. The most frequently observed O^{1-} center is $O^{1-}/2^{27}Al$. It consists of a spectrum of 11 more or less equidistant EPR signals due to Al–O^{1-}–Al bridges (nuclear spin I of ^{27}Al, $I = 5/2$, natural abundance of ^{27}Al 100%). The pattern demonstrates a violation of the principle of Loewenstein (1954). It was observed first in albite by Ioffe and Yanchevskaya (1968) and in microcline by Marfunin and Bershov (1970). It was also found in alkali feldspars including albite by Speit and Lehmann (1982). Hofmeister and Rossman (1985) detected 13 apparent SHF lines in a dehydrated gray microcline powder and interpreted that spectrum in terms of a superposition of two nonequivalent $O^{1-}/2^{27}Al$ centers.

2. Another O^{1-} spectrum in feldspars consists of six equidistant lines due to $O^{1-}/^{27}Al$ interaction. It is probably produced by an unknown point defect in the local crystallographic environment. A possible defect could be substitution of Al for Si in a structural Si–O–Si bridge. Matyash et al. (1981, 1982) observed that spectrum first in microcline. Speit and Lehmann (1982) irradiated a "sunstone" (plagioclase) at 77 K and took EPR spectra subsequently at the same temperature without warming up to 295 K between irradiation and the EPR experiment. They found an $O^{1-}/^{27}Al$ center that, after heating to 295 K and subsequent recooling, apparently "transformed" to an $O^{1-}/2^{27}Al$ center.

Hofmeister and Rossman (1985) reported a sextet apparently due to $O^{1-}/^{27}Al$ in natural and irradiated microcline. A of the SHF interaction due to ^{27}Al in alkali feldspar is expected to be of the order of 25 MHz. A of Hofmeister and Rossman (1985), however, is about ten times larger (cf. their Fig. 4a). The pattern is, therefore, rather from an Mn^{2+} center (^{55}Mn, $I = 5/2$, natural abundance of ^{55}Mn 100%, $A \approx 250$ MHz), e.g., as observed in natural oligoclase (Matyash et al., 1981) and in natural albite (Petrov et al., 1989). In irradiated microcline, of course, the center could also be assigned to $O^{1-}/^{55}Mn^{2+}$. This was observed, for example, in topaz (Petrov, 1983). For unambiguous interpretation, a single-crystal study is needed.

3. A spectrum that exhibits four equidistant lines due to $O^{1-}/^{23}Na$ ($I = 3/2$, natural abundance of ^{23}Na 100%) was described in microcline by Marfunin and Bershov (1970).

4. An O^{1-} single line together with a doublet due to $O^{1-}/^{207}Pb$ ($I = 1/2$, natural abundance of ^{207}Pb 22.6%), was found in microcline (amazonite) by Marfunin and Bershov (1970) and Speit and Lehmann (1982).

5. A doublet probably due to $O^{1-}/^{107+109}Ag$ (for both isotopes $I = 1/2$, natural abundance of $^{107+109}Ag$ 100%), was noted in microcline by Marfunin and Bershov (1970).

6. A paramagnetic center $SiO_3\boxdot^{3-}/^{27}Al$ (tetrahedron with an oxygen vacancy, $\boxdot$) with 6 SHFS components from an Al atom nearby was found in microcline by Matyash et al. (1981, 1982).

7. $O^{1-}/[Si,M^{2+}]$ centers exhibiting one sharp single line without resolved SHFS were reported to occur in microcline, oligoclase, labradorite, bytownite, and anorthite (Marfunin and Bershov, 1970; Speit and Lehmann, 1982; Matyash et al., 1981, 1982). These were assigned to Si–O–M^{2+} bridges, $O^{1-}/[Si, M^{2+}]$, assuming that Si or Al at an adjacent tetrahedral position is replaced by a bivalent cation M^{2+}.

8. In polycrystalline samples of three "hydrous" microclines (amazonite) and sanidine, Hofmeister and Rossman (1985) observed a superposition of a sextet, H_I, and a single line, H_{II}, which were interpreted as two distinct "$[SiO_4/K^+]^{2+}$" centers. H_I disappeared after dehydration. Inspection of their Figure 4b suggests, however, an alternative interpretation: H_I is not a sextet; it consists of three doublets arising from three nonequivalent protons as a result of averaging of the three eigenvectors of g_{xx}, g_{yy}, and g_{zz} and of A_{xx}, A_{yy}, and A_{zz} over the powder (L. V. Bershov, personal communication). The "sextet" is, therefore, due to one O^{1-} center with three satellite doublets from three protons that disappear after dehydration.

9. A $PO_3\boxdot^{2-}$ center can be identified in Figure 4a of Hofmeister and Rossman (1985) who studied the EPR spectrum of powdered microcline. The four-line pattern was labeled as "unknown" by the authors. It apparently possesses a HF coupling constant of $A_{iso} \approx 1820$ MHz because of an interaction with ^{31}P ($I = 1/2$, natural abundance 100%). The two doublets are unresolved for $A_{xx} = A_{yy}$ ($A_\perp$) and A_{zz} ($A_\parallel$) in the case of axial symmetry of the PO_3^{2-} complex in powder samples. In topaz single crystals, the two doublets arise from two distinct PO_3^{2-} complexes at two crystallographically nonequivalent tetrahedral positions (Petrov, 1983).

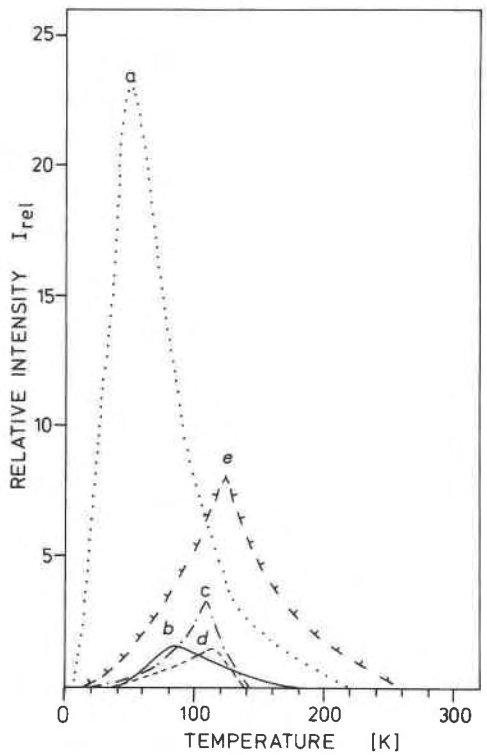

Fig. 1. Temperature-dependence of the line intensities of four O^{1-} centers in albite at controlled measuring conditions. (a) $O^{1-}/2^{27}Al$, center 1; (b) $O^{1-}/2^{27}Al$, center 2; (c) $O^{1-}/^{27}Al \times 2^{23}Na$, SHFS intensity of ^{27}Al; (d) same center as (c), SHFS intensity of ^{23}Na; (e) $O^{1-}/[Si,M^{2+}]$ center. The temperature dependence was measured for different orientations of each center with respect to **B** to account for optimum resolution. The line intensities of the centers are strongly anisotropic; the effective intensities plotted in the figure cannot be referred to the frequency of the center in the crystal. The following crystal orientations were used: for (a), Rotation 1, $\theta = 123°$; for (b), same as (a); for (c), Rotation 1, $\theta = 20°$; for (d), Rotation 2, $\theta = 140°$; for (e), same as (a).

Samples

The crystals used for the experiments were from Amelia Court House, Virginia, U.S.A. (the same crystals as used by Petrov et al., 1989). They had large parts that were untwinned, optically transparent, quite homogeneous, and colorless. The volumes of untwinned single-crystal fragments cut for EPR experiments were about 1.5 mm^3.

Experimental details

Before carrying out the EPR experiments, the crystals were exposed to X-ray (Cu$K\alpha$, 16 mA, 35 kV) radiation for 3 h. The EPR studies were performed generally within a few days after irradiation. Care was taken that the samples were not exposed to light over a longer period of time. The spectra were recorded in the X band (~9.2 GHz) as described in Petrov et al. (1989).

For a description of the EPR spectra, the orthogonal laboratory system $\mathbf{X}^0$, $\mathbf{Y}^0$, $\mathbf{Z}^0$ was used, $\mathbf{Z}^0$ being the axis of rotation of the crystal perpendicular to **B** and $\mathbf{X}^0$ being parallel to **B**. The observed EPR signals were labeled by their g values, g_{eff}, being defined by the relation

$$h\nu = g_{eff}(\theta)\beta\mathbf{B}. \quad (1)$$

Here **B** is the field at which resonance occurs, ν is the resonance frequency, β is the Bohr magneton, h is Planck's constant, **g** is the electronic g "factor," i.e., a tensor of second rank with the eigenvalues g_{xx}, g_{yy}, g_{zz}. The factor $g_{eff}(\theta)$ is the value of **g** in the direction of $\mathbf{X}^0$, and θ is the angle between crystallographic **a** or **c*** according to the rotations defined below and $\mathbf{X}^0$.

The crystals were aligned by use of a goniometer in the spectrometer. They were rotated clockwise around $\mathbf{Z}^0$ at different temperatures within the cryostat, and spectra were recorded every 10°; over critical ranges spectra were recorded every 1°–5°. The following rotations were used:

$$+\mathbf{a} \parallel +\mathbf{Z}^0, \quad +\mathbf{c}^* \parallel +\mathbf{X}^0 \quad (\theta = 0), \quad (1)$$
$$+\mathbf{c}^* \parallel +\mathbf{Z}^0, \quad +\mathbf{a} \parallel +\mathbf{X}^0 \quad (\theta = 0), \quad (2)$$
$$+\mathbf{b}^* \parallel +\mathbf{Z}^0, \quad +\mathbf{a} \parallel +\mathbf{X}^0 \quad (\theta = 0), \quad (3)$$

where **a**, **b***, and **c*** refer to the crystallographic axes of albite.

Considering the three rotations, only Rotations 1 and 2 are exactly orthogonal to each other. Rotation 3 is oblique to Rotations 1 and 2 by about 3°. Rotations 1 and 2 and a corrected Rotation 3 were used to determine the eigenvalues and direction cosines of the **g** tensor from the angular dependences of the spectra by conventional procedures (Wertz and Bolton, 1972).

Results

At room temperature, no O^{1-} hole centers could be detected in natural or irradiated crystals of our albite with EPR, either in the X band (~9.2 GHz) or in the Q band (~35 GHz). For observation of O^{1-} at low temperatures, it was necessary to irradiate the crystals first with X-rays. After irradiation, the colorless crystals became brownish gray. Inspection of the records of irradiated crystals taken at different temperatures between 5 and 295 K revealed that several crystallographically distinct centers of O^{1-} were present that could be studied only at temperatures lower than ~250 K. The intensities of the lines depend critically on the orientation of the crystal with respect to B. Each O^{1-} center showed a characteristic temperature T_m, at which the intensity was maximum, T_m being between 60 and 115 K. The dependence of the line intensities of the centers on temperature is shown in Figure 1. The spectra of all centers were identical in each irradiated crystal fragment of our specimen of Amelia albite, exhibiting identical **g** and **A** values and intensities. A resonant absorption line at $g < 2$ that was due to electron centers (e.g., Ti^{3+} or $SiO_3\square^{3-}$) could not be seen. The spectra did not reveal any twinning of the crystal fragment used. The absence of twinning, e.g., after the albite or pericline law,

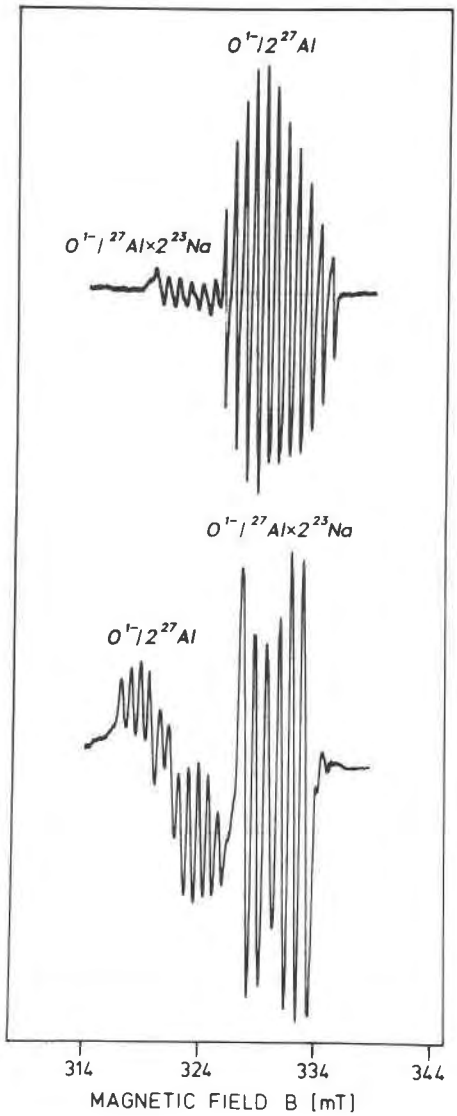

Fig. 2. SHFS splitting of $O^{1-}/2^{27}Al$ (center 1) and $O^{1-}/^{27}Al \times 2^{23}Na$ in Amelia albite (upper spectrum, Rotation 1, $\theta = 10°$; lower spectrum, Rotation 2, $\theta = 120°$), $\nu = 9.2436$ GHz, and $T = 80$ K. In the upper spectrum, the 11-line SHFS of the $O^{1-}/2^{27}Al$ center occurs at the higher **B**, and the 6-line SHFS of the $O^{1-}/^{27}Al \times 2^{23}Na$ center occurs at the lower **B**. In the lower spectrum, the 11-line pattern occurs at the lower **B**, and the sextet at the higher **B**. The SHFS of ^{23}Na is not resolved in the two spectra. The two spectra demonstrate also the orientational anisotropy of the intensities of the lines.

was also confirmed by optical inspection. This simplified the crystallographic analysis of the centers.

Six different O^{1-} EPR centers could be identified in our albite from their distinct **g** values and SHFS line intensities, depending on T_m and crystal orientation with respect to **B**.

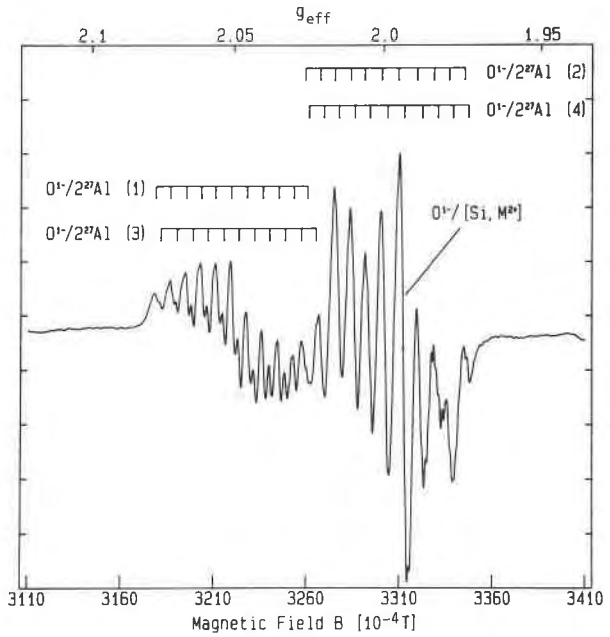

Fig. 3. SHFS of the four distinct $O^{1-}/2^{27}Al$ centers 1, 2, 3, and 4, Rotation 1, $\theta = 102°$, $\nu = 9.2424$ GHz, $T = 60$ K.

$O^{1-}/2^{27}Al$ centers

The $O^{1-}/2^{27}Al$ hole center can be identified by its characteristic SHFS spectrum of 11 quasi-equidistant lines, exhibiting intensities according to the approximate ratio 1:2:3:4:5:6:5:4:3:2:1. This center was observed mainly between 5 and 220 K. The temperature of maximum intensity was $T_m \approx 60$ K. A typical spectrum is shown in Figure 2. A SHFS pattern of this type is due to the interaction of an unpaired electron ($S = 1/2$) with two adjacent nuclei ^{27}Al ($I = 5/2$) that are separated from the hole center by about the same distance. The angular dependence of the spectrum when the crystal is rotated around $\mathbf{Z}^0$ is described by the spin-Hamiltonian:

$$\mathbf{H} = \beta \mathbf{B} \mathbf{g} \mathbf{S} + \sum_{i=1}^{2} \mathbf{S} \mathbf{A}_{Al} \mathbf{I}_{Al}. \qquad (2)$$

Here **A** is the tensor of the SHF interaction between **S** of O^{1-} and **I** of ^{27}Al. In Equation 2 the effect of the nuclear quadrupole interaction of ^{27}Al is neglected. Its consideration would produce a small deviation from the equidistant field positions of the 11 lines within the spectrum. That deviation was within our experimental error and was ignored in our study.

Careful inspection of the region around $g = 2$ revealed that for certain orientations of the crystal with respect to **B**, more than 11 lines were present, indicating superposition of several 11-line spectra that must have different angular dependencies. The pattern showed overlap over a large range of angles, the displacements of the lines being just a few millitesla. It was possible to identify four crystallographically distinct $O^{1-}/2^{27}Al$ centers 1, 2, 3, and

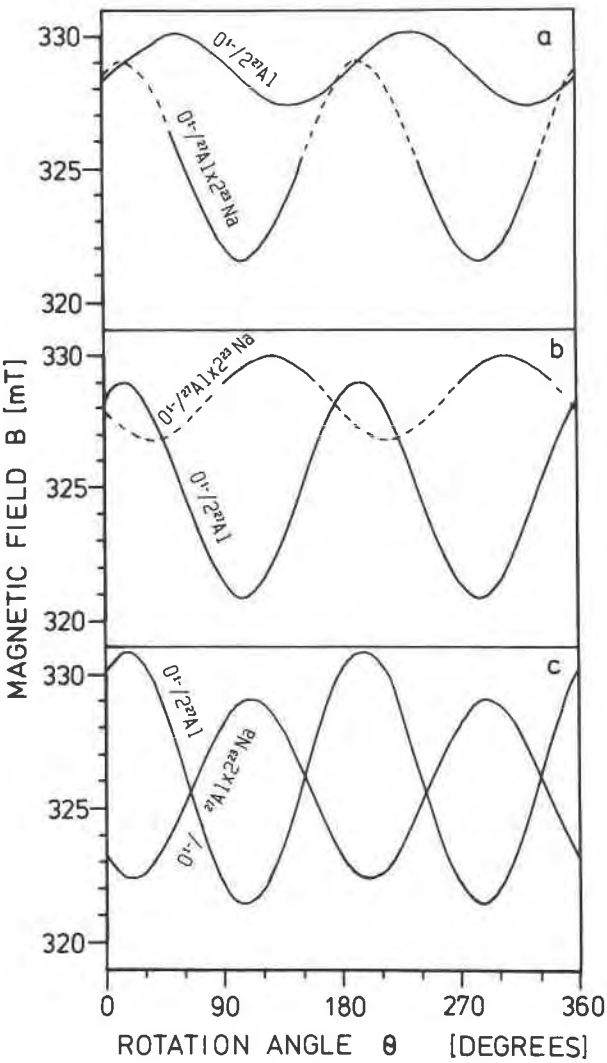

Fig. 4. Field dependence of the center position of the 11-line SHFS of the $O^{1-}/2^{27}Al$ and the 6-line SHFS of the $O^{1-}/^{27}Al \times 2^{23}Na$ centers at 20 and 60 K, respectively. (**a**) Rotation 3, (**b**) Rotation 2, (**c**) Rotation 1. The minimum field values mark the projections of the respective g_{zz} eigenvectors. Dashed lines: regions of incomplete resolution because of pattern overlap.

4 (Fig. 3), and their spectra exhibited an intensity ratio of about 2:2:1:1. The estimated concentration of center 1 is at least 1×10^{-4} per formula unit $NaAlSi_3O_8$.

The angular dependence of the center position of the spectrum of center 1 on crystal orientation with respect to **B** is shown in Figure 4. The eigenvalues and eigenvectors of the **g** tensors of the centers 1, 2, and 3 are presented in Table 1. A stereographic projection of the eigenvectors is given in Figure 5. For the weak center 4, it was not possible to determine the tensors exactly because of the overlap of the lines with the intensity patterns of 1 and 2 over a large range of angles.

The data of Table 1 may be compared with the eigen-

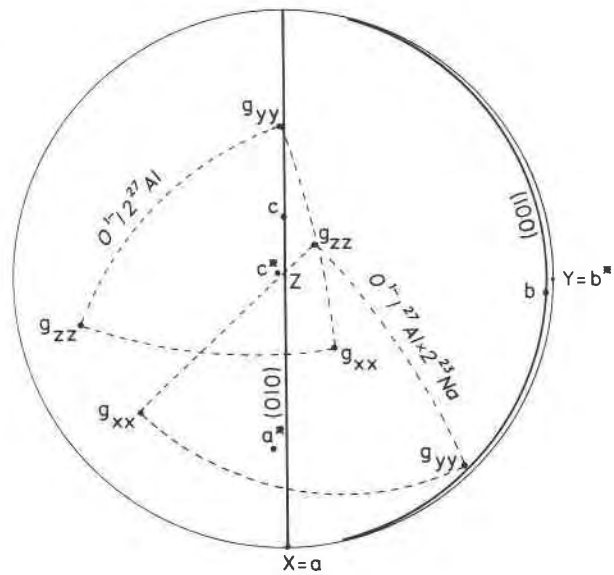

Fig. 5. Stereographic projection of the **g** eigenvectors of the $O^{1-}/2^{27}Al$ (center 1) and $O^{1-}/^{27}Al \times 2^{23}Na$ centers. The values of the eigenvectors of $O^{1-}/2^{27}Al$ (center 2) are similar to those of $O^{1-}/^{27}Al \times 2^{23}Na$; they are listed in Table 1, but not plotted in this figure.

values of an $O^{1-}/2^{27}Al$ center in albite described by Ioffe and Yanchevskaya (1968), Marfunin and Bershov (1970), and Speit and Lehmann (1982). The eigenvectors were not reported in those papers. The SHF tensor **A** in our case exhibits a small anisotropy. Its average value is $A_{iso} = 25$ MHz. The individual peak-to-peak widths, ΔB_{pp}, of the lines are $\Delta B_{pp} = 4 \pm 0.5 \times 10^{-4}$ T. ΔB_{pp} as well as A_{iso} did not change between 5 and 220 K. At temperatures higher than ~150 K, the **g** tensors of the $O^{1-}/2^{27}Al$ centers became quasi-isotropic, and the spectra of the four centers could no longer be distinguished.

$O^{1-}/^{27}Al \times 2^{23}Na$ center

In addition to the 11-line spectra of the $O^{1-}/2^{27}Al$ hole centers, a distinct hole center of O^{1-} was found that exhibits six main quasi-equidistant lines of equal intensity. This center was observed mainly between 20 and 120 K. The temperature of maximum intensity, T_m, was ~110 K. The line intensity depends strongly on the orientation of the crystal. This dependence is shown in Figure 2 for two different orientations of the crystal with respect to **B**. The width, $\Delta^{27}B_{pp}$, of a SHFS line is about $6 \pm 0.5 \times 10^{-4}$ T.

For certain orientations, especially in the temperature range 30–140 K, each of the six lines is additionally split into a subpattern of seven approximately equidistant lines, the width, $\Delta^{23}B_{pp}$, of a single line being about $0.8 \pm 0.2 \times 10^{-4}$ T. The total number of lines of the pattern is, therefore, 42 as shown in Figure 6. The intensity ratio of the seven-line subpattern appears to be near 1:2:3:4:3:2:1 (cf. Fig. 6). The seven-line splitting can be seen best in

TABLE 1. Eigenvalues and direction cosines of the **g** tensors for the $O^{1-}/2^{27}Al$ center in albite; **X** ∥ + **a**; **Y** ∥ + **b***; **Z** ⊥ + **a**, ∥ (010)

Center	Eigenvalues*	T (K)	Direction cosines X	Y	Z	Reference
c_O $O^{1-}/2^{27}Al(1)$	g_{xx} = 2.000(6)	20	0.53	0.34	0.78	This work
	g_{yy} = 2.023(2)		−0.82	−0.002	0.57	
	g_{zz} = 2.065(0)		−0.19	0.94	−0.28	
c_O $O^{1-}/2^{27}Al(1)$	g_{xx} = 1.998(1)	60	0.44	0.39	0.81	This work
	g_{yy} = 2.026(2)		−0.88	0.02	0.47	
	g_{zz} = 2.077(8)		−0.17	0.92	−0.35	
d_O $O^{1-}/2^{27}Al(2)$	g_{xx} = 2.009(0)	60	0.57	0.66	0.50	This work
	g_{yy} = 2.013(7)		0.70	−0.70	0.13	
	g_{zz} = 2.056(2)		−0.44	−0.27	0.86	
c_m $O^{1-}/2^{27}Al(3)$	g_{xx} = 1.998(5)	60	0.50	0.38	0.77	This work
	g_{yy} = 2.026(2)		−0.85	0.03	0.53	
	g_{zz} = 2.076(1)		−0.18	0.92	−0.34	
a''_1 (c_O?) $O^{1-}/2^{27}Al$	g_{xx} = 2.003	77	not reported			Ioffe and Yanchevskaya (1968)
	g_{yy} = 2.010					
	g_{zz} = 2.067					
c_O(?) $O^{1-}/2^{27}Al$	g_{xx} = 2.0044	78	not reported			Marfunin and Bershov (1970)
	—					
	g_{zz} = 2.075					
b_O $O^{1-}/2^{27}Al$	g_{xx} = 2.0044	77	not reported			Speit and Lehmann (1982)
	g_{yy} = 2.0109					
	g_{zz} = 2.0347					

* In the literature, g values of single-crystal measurements were often calculated up to fourth order. A small misorientation changes the g values in angular-dependent spectra of single crystals. In our albite, a misorientation of 0.5° changes the g values by ±0.0006. Such a misorientation cannot be excluded for single-crystal measurements.

Rotation 2. In other directions, the splitting cannot be observed well because of overlap with other lines.

The six-line spectrum is interpreted in terms of an SHF interaction of O^{1-} with one neighboring ^{27}Al (I = 5/2), resulting in $2I + 1 = 6$ lines. The additional splitting into seven lines is due to two additional ^{23}Na (I = 3/2) neighbors, yielding $2nI + 1 = 7$ lines (n = 2). The angular dependence of the EPR spectrum (42 lines) may be described by

$$\mathbf{H} = \beta\mathbf{BgS} + \mathbf{SA}_{Al}\mathbf{I}_{Al} + \sum_{i=1}^{2} \mathbf{SA}_{Na}\mathbf{I}_{Na}. \quad (3)$$

The eigenvalues and eigenvectors of **g** were obtained from the data plotted in Figure 4 and listed in Table 2. They may be compared with those of a similar six-line center described for microcline by Matyash et al. (1982). Our eigenvectors are projected in Figure 5. The SHF tensor $^{27}\mathbf{A}$ (cf. Eq. 3) is of little anisotropy, the mean value of $^{27}\mathbf{A}$ being $^{27}A_{iso}$ = 25 MHz. The mean eigenvalue of the two SHF tensors $^{23}\mathbf{A}$ could be estimated from certain orientations to be approximately $^{23}A \approx 4.2$ MHz. $\Delta^{27}B_{pp}$ and $\Delta^{23}B_{pp}$ as well as ^{27}A and ^{23}A did not change between 5 and 220 K.

Depending on orientation, at temperatures between 70 and 150 K, the $O^{1-}/^{27}Al \times 2^{23}Na$ sextet was more and more covered by additional lines of one $O^{1-}/2^{27}Al$ center, which became relatively more intense. At temperatures higher than 150 K, the sextet disappeared, and only the 11-line multiplet could be seen; the **g** tensor of the $O^{1-}/2^{27}Al$ center became quasi-isotropic.

O^{1-}/[Si,M²] center

An EPR hole center of O^{1-} was found that consisted of one single line near g = 2, its line width, ΔB_{pp}, being 6 ± 0.5 × 10^{-4} T. No SHFS could be detected in the temperature range over which the center was observed (10–260 K). The temperature of maximum intensity was $T_m \approx$ 115 K. The angular dependence of the spectrum for crystal rotation around $\mathbf{Z}^0$ is described by the first term, $\beta\mathbf{BgS}$, of Equation 2. The eigenvalues, eigenvectors, and the cosines of direction of the **g** tensor at this single-line O^{1-} center determined by use of Equation 2 are listed in Table 3.

Obviously, the center must be located at an oxygen position that possesses only silicons as neighboring tetrahedral atoms. Its field dependence on crystal orientation with respect to **B** is similar to that of the $O^{1-}/^{27}Al \times 2^{23}Na$ center, although it is clearly independent of the latter. Centers of this type were described to exist in irradiated microcline, labradorite, and oligoclase (Marfunin and Bershov, 1970; Speit and Lehmann, 1982; Matyash et al., 1982). The data of the **g** tensor of our single-line hole center in albite may be compared with those of that center reported for other feldspars in Table 3.

DISCUSSION

The primary aim of this section is to discuss location and state of bonding of the observed O^{1-} ions as described above. Conclusions on the assignments to crystallographic positions will be based mainly on the direc-

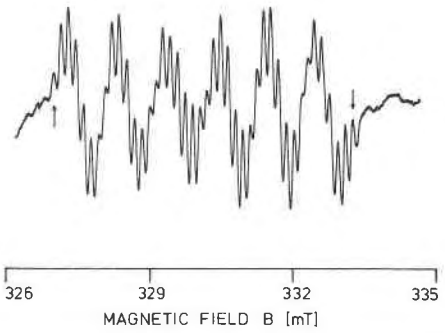

Fig. 6. Spectrum of the 42-line SHFS of the $O^{1-}/^{27}Al \times 2^{23}Na$ center in Amelia albite, $\nu = 9.2443$ GHz, and $T = 89$ K. The 6 ^{27}Al line groups and the 42 ^{23}Na lines (between the two arrows) are about equally separated from each other.

tion of g_{zz} of the **g** tensor and the SHFS splitting due to nuclear moments at ions in adjacent positions.

$O^{1-}/2^{27}Al$ centers

Centers of this type may be formed where two adjacent tetrahedral positions on either side of an oxygen atom are occupied by Al atoms, building an Al–O–Al bridge. The generally metastable $2p^5$ configuration of O^{1-} is relatively stabilized by reducing the local charge unbalance of the Al^{3+}–$O^{2-}(2p^6)$–Al^{3+} configuration. If the distribution of Al and Si over the four nonequivalent tetrahedral positions in albite is ideally ordered, i.e., if all Al atoms are located at the position T1(O) and all Si atoms at T1(m), T2(O), and T2(m), there will be no Al–O–Al bridges. The optical properties (e.g., the optical angle $2V$) as well as the cell dimensions of Amelia albite (Petrov et al., 1989) are indicative of nominally complete Al-Si order. It is generally assumed that Al-Si disorder in feldspars is formed by sustaining a high degree of short-range order. For example, if an Al atom is located at a T1(m) position, the probability that the adjacent T1(O) position is occupied by Si should be comparatively high. If the degree of disorder is small, a correlated Al-Si distribution may be constructed, yielding quasi-perfect short-range order without Al–O–Al bridges. However, the existence of paramagnetic $O^{1-}/2^{27}Al$ centers proves that short-range order is obviously not complete. Most probably, only a very small fraction of Al^{3+}–O^{2-}–Al^{3+} bridges may be occupied by a hole center and thus "visible" in the EPR spectrum. It would be interesting to study the critical temperature, T_m, of maximum intensity (cf. Fig. 1) more precisely as T_m is expected to depend on the frequency of Al–O–Al bridges in the albite crystal: a higher frequency should be associated with a lower activation energy for intracrystalline exchange of the electron hole and, therefore, yield a lower T_m.

TABLE 2. Eigenvalues and direction cosines of the **g** tensors for $O^{1-} / \sum_{i=1}^{m} Y_i \times \sum_{j=1}^{n} Z_j$ centers ($Y = {}^{27}Al$; $Z = {}^{1}H$, ^{7}Li, ^{23}Na) in feldspar and quartz; $\mathbf{X} \parallel +\mathbf{a}$; $\mathbf{Y} \parallel +\mathbf{b}^*$; $\mathbf{Z} \perp +\mathbf{a}$, $\parallel (010)$

Mineral	Center	Eigenvalues*	T (K)	Direction cosines			Reference
				X	Y	Z	
Albite	a'$_1$ $O^{1-}/^{27}Al \times 2^{23}Na$	$g_{xx} = 2.006(8)$ $g_{yy} = 2.027(5)$ $g_{zz} = 2.056(4)$	60	−0.54 0.82 −0.20	0.77 0.57 0.29	−0.36 −0.02 0.93	This work
Microcline	a'$_1$ $O^{1-}/^{27}Al$	$g_{xx} = 1.9911$ $g_{yy} = 2.0225$ $g_{zz} = 2.0505$	77	±0.66 +0.64 +0.39	+0.67 ±0.74 ±0.07	±0.34 −0.22 +0.92	Matyash et al. (1982)
Quartz	$O^{1-}/^{27}Al$	$g_{xx} = 2.0024$ $g_{yy} = 2.0091$ $g_{zz} = 2.0614$	77				Schnadt and Schneider (1970)
Quartz	$O^{1-}/^{27}Al$	$g_{xx} = 2.0019$ $g_{yy} = 2.0085$ $g_{zz} = 2.0602$	35				Nuttal and Weil (1981)
Quartz	$O^{1-}/^{27}Al \times {}^{1}H$	$g_{xx} = 2.0034$ $g_{yy} = 2.0093$ $g_{zz} = 2.0581$	77				Matyash et al. (1987)
Quartz	$O^{1-}/^{27}Al \times {}^{7}Li$	$g_{xx} = 2.0033$ $g_{yy} = 2.0083$ $g_{zz} = 2.0618$	77				Matyash et al. (1987)
Quartz	$O^{1-}/^{27}Al \times {}^{23}Na$	$g_{xx} = 2.0021$ $g_{yy} = 2.0096$ $g_{zz} = 2.0437$	77				Matyash et al. (1987)
Citrine	$O^{1-}/^{27}Al$	$g_{xx} = 2.00346$ $g_{yy} = 2.00925$ $g_{zz} = 2.03408$	77				Maschmeyer et al. (1980)

* See Table 1.

TABLE 3. Eigenvalues and direction cosines of the **g** tensor for the $O^{1-}/[Si,M^{2+}]$ center in feldspar; **X** ∥ + **a**; **Y** ∥ + **b***; **Z** ⊥ + **a**, ∥ (010)

Feldspar	Eigenvalues*	T (K)	Direction cosines			Reference
			X	Y	Z	
Albite	$g_{xx} = 2.007(7)$	60	0.89	0.43	−0.13	This work
	$g_{yy} = 2.022(8)$		0.45	−0.84	0.31	
	$g_{zz} = 2.061(8)$		−0.02	0.34	0.94	
Amazonite	$g_{xx} = 2.0036$	78		not reported		Marfunin and Bershov (1970)
	—					
	$g_{zz} = 2.0599$					
Labradorite, oligoclase	$g_{xx} = 1.9917$	77		not reported		Speit and Lehmann (1982)
	$g_{yy} = 2.0101$					
	$g_{zz} = 2.0193$					
Amazonite	$g_{xx} = 2.0040$	77		not reported		Speit and Lehmann (1982)
	$g_{yy} = 2.0098$					
	$g_{zz} = 2.0123$					
Microcline	$g_{xx} = 1.999$	77	0.99	0.08	−0.07	Matyash et al. (1982)
	$g_{yy} = 2.010$		−0.09	0.98	−0.19	
	$g_{zz} = 2.054$		0.05	0.20	0.98	

* See Table 1.

There are 32 T–O–T bridges in the base-centered unit cell of albite that may be potential electron-hole centers. Eight of them are distinct from the point of view of EPR, the others being equivalent by translation or inversion symmetry and, therefore, indistinguishable in the EPR spectrum. They are

$$T1(O)–O_{A1}–T1(m),$$
$$T1(O)–O_{B(O)}–T2(O),$$
$$T1(O)–O_{C(O)}–T2(m),$$
$$T1(O)–O_{D(O)}–T2(m),$$
$$T1(m)–O_{D(m)}–T2(O),$$
$$T1(m)–O_{C(m)}–T2(O),$$
$$T1(m)–O_{B(m)}–T2(m),$$
$$T2(O)–O_{A2}–T2(m).$$

Here, the notation of Megaw (1956) is used for identification of the atomic positions. An assignment of the observed centers to the particular T–O–T bridges may be made from the eigenvector g_{zz} of the **g** tensor, assuming that this vector is approximately parallel to the T–T direction of the ^{27}Al nuclei that produce the SHFS splitting. Comparison of the eigenvectors of the centers 1, 2, 3, and 4 with the T–T directions of the eight T–O–T bridges yields a most probable assignment of the two intense centers 1 and 2 to oxygens at the C(O) and D(O) positions, respectively, and an assignment of the weak centers 3 and 4 to C(m) and D(m). Unfortunately, the **g** tensor could be determined precisely for centers 1, 2, and 3 only. For center 4, the overlap of the multiplet with those of other centers was great for many crystal orientations with respect to **B** so that a complete tensor determination was not possible. The assignment of center 4 to D(m) was concluded from interpolation over incompletely resolved regions of the crystal rotations around $\mathbf{Z}^0$.

According to Marfunin (1979), $O^{1-}/2^{27}Al$ centers are expected to occur mainly at the oxygen positions A1, B(O), C(O), and D(O), i.e., at positions bridging the T1(O) position with adjacent tetrahedra, whereas the oxygen positions A2, B(m), C(m), and D(m) should be less probable since they bridge tetrahedra occupied by Si in the case of complete Al-Si order. It should be noted, however, that an $O^{1-}/2^{27}Al$ center at C(O) or D(O) requires Al–O–Al–O–Al bridges in a well-ordered crystal: a "double violation" of the principle of Loewenstein. This is avoided at A1 and B(O). In any case, any small, local Al-Si disorder will change the probabilities derived from structural inspection as above. Experimental assignment of the center to C(O) and D(O) based on the eigenvectors of the **g** tensors for the intense centers 1 and 2 implies occupation of the adjacent T1(O) tetrahedra by Si and not Al. A very small degree of Al-Si disorder, i.e., a site occupancy of Al for T1(O) somewhat smaller than one as generally expected for natural low albite should enhance the frequency of the centers 1 and 2. Their intensities should increase with increasing disorder. The estimated concentration of the four centers is 2×10^{-4} to 3×10^{-4} per formula unit.

For an unambiguous description of O^{1-} centers in feldspar, a notation related to crystal structure is convenient. For this the centers 1, 2, 3, and 4 are designated as c_O, d_O, c_m, and d_m, referring to the oxygen positions C(O), D(O), C(m), and D(m), respectively. $O^{1-}_{B(O)}$ in microcline (Speit and Lehmann, 1982) is labeled b_O; $O^{1-}/2^{27}Al$ at oxygen position A1, a_i'' and $O^{1-}/^{27}Al \times 2^{23}Na$, a_i'.

The existence of c_m and d_m centers requires simultaneous replacement of two Si by Al at adjacent T1(m) and T2(O) positions. We have no explanation why no a_i'' center with two adjacent aluminums could be observed at the A1 position, which possesses T1(O) nominally occupied by Al as neighbor. Al–A1–Al bridges have the highest probability from the point of view of geometrical crystal structure. Ioffe and Yanchevskaya (1968) observed a_i'' in an irradiated natural albite crystal, but it is

not clear from their paper whether this interpretation is based on experimental determination of the **g** tensor or speculation from crystal structure.

Speit and Lehmann (1982) pointed out that hole centers will prefer the position that possesses the widest separation from adjacent cations. In crystals of both "sunstone" (plagioclase) and microcline, they found a b_O center that exhibits the greatest T–O separation. In microcline, however, they detected a second center that was of very low intensity and could not be assigned by its **g** tensor. The T–O distances of the T1(O), T1(m), T2(O), and T2(m) tetrahedra in albite appear to be so similar that no strong preference of a hole center for a particular oxygen position may be expected.

All O^{1-} centers in albite could be observed only at temperatures lower than 260 K, similar to the $O^{1-}/2^{27}Al$ center in smoky quartz. At higher temperatures, the thermal exchange of the holes between various oxygen positions is apparently so rapid that they could no longer be resolved in the EPR spectrum.

In quartz, where T–O–T angles are ~144°, the local crystal-field symmetry at the site of the O^{1-} center is nearly axial. The eigenvalues of the **g** tensor are $g_{xx} \approx g_{yy} < g_{zz}$ (cf. Table 2). In albite, where $T–D_{(O)}–T$ angles are ~134°, the eigenvalues of center d_O are $g_{xx} < g_{yy} \ll g_{zz}$, and where $T–C_{(O)}–T$ angles are ~129°, the eigenvalues of center c_O are $g_{xx} \ll g_{yy} \ll g_{zz}$ (cf. Table 1). The crystal-field symmetry at the sites of these centers is quasi-orthorhombic or lower.

The SHF coupling constant of the $O^{1-}/2^{27}Al$ centers, $A \approx 25$ MHz, is nearly independent of orientation and about the same in all feldspars studied (Marfunin and Bershov, 1970; Matyash et al., 1981; Speit and Lehmann, 1982). It corresponds to an *s*-electron density of 0.006 e at the ^{27}Al position (Morton and Preston, 1978). This is about 50% more than values reported for smoky quartz (Barker, 1975) and about three times as great as values for citrine quartz (Maschmeyer et al., 1980). Comparison of the mean values of **A** of centers in quartz and feldspar reveals an increase of covalent participation in the Al–O bond in feldspar of more than 50% over that in quartz.

Whereas the intensity of the resonant lines are strongly dependent on temperature, the widths of the lines are nearly independent of temperature between 5 and 220 K, within experimental error. This finding indicates that the life time of the excited state does not influence the line width ΔB_{pp}. The large line widths observed in feldspar compared to those in quartz must be due to other phenomena, most probably to unresolved SHF interactions with nuclear magnetic moments of adjacent atoms (e.g., Na, Al; cf. next section) and/or some disorder in the Al-Si occupancy of adjacent tetrahedra.

The high mobility of the defect electrons at room temperature is somewhat surprising since the oxygen positions of the Al and Si tetrahedra in albite are not equivalent by symmetry. It seems, however, that because of the small tetrahedral deformations, the oxygen positions are quasi-equivalent from the point of view of exchange energy. Moreover, low activation energies allow thermal exchange at room temperature. At lower temperatures, the unpaired electron is "frozen" at a preferred oxygen position and gives rise to a well-resolved EPR spectrum. Below 60 K, the line intensity decreases gradually; it disappears at 5 K (Fig. 1). These effects cannot be due to a relaxation process since the line width does not change with decreasing temperature. An explanation could be a gradual change in structure at low temperatures. If AlO_4 tetrahedra change their geometry, the depth of electron traps of different O^{2-} atoms may be changed so that other O^{2-} ions become energetically more favorable, representing deeper electron traps. If the new traps do not possess adjacent ^{27}Al, no SHFS occurs. For low albite, Winter et al. (1977) showed that the bond angles as a function of temperature display a quite linear fit, the O–T–O and T–O–T changing by more than 0.5° and 3°, respectively. Optically detected magnetic resonance at low temperatures and ENDOR experiments may provide more information.

$O^{1-}/^{27}Al \times 2^{23}Na$ center

As shown in Figure 7, the direction of g_{zz} of this center is approximately parallel to the direction of the line connecting adjacent T1(O) and T1(m) positions. The center should, therefore, be assigned to the oxygen A1 position and is designated as a_1'. Its concentration is at least 1×10^{-4} per formula unit. The T1(O)–A1 distance, $d = 1.7472$ Å (Harlow and Brown, 1980), is the greatest T–O distance in the structure of albite as well as microcline. This great distance may particularly stabilize the hole on A1. Similar centers, designated as $Al/Na^+–O^{1-}$ ($O^{1-}/^{27}Al \times {}^{23}Na$ according to our notation), produced in quartz by artificial irradiation were described by Nuttal and Weil (1981) and Matyash et al. (1987). The centers in quartz could be observed at low temperatures only, as in feldspar. For the $O^-/^{27}Al$ center in quartz, O'Brien (1955) found that the hole is captured at the nonbonding orbital of an oxygen ion in an Al tetrahedron at the "long" or "short" Al–O bond. As a result, two center modifications are formed (Schnadt and Schneider, 1970), and at a temperature above 120 K, the hole is distributed over four oxygen ions bound to an Al (Schnadt and Räuber, 1971).

The a_1' center in feldspar is probably formed by simultaneous substitution of Al for Si at T1(m) and of Si for Al at T1(O). Unlike in quartz, there is no direct evidence for charge imbalance, either by violation of the rule of Loewenstein or by the presence of any other charge defect at adjacent T or M positions, although a stabilizing defect may be present that does not perturb the SHFS of the center and, therefore, cannot be identified by EPR.

The total SHFS splitting of the a_1' spectrum into 42 approximately equidistant lines requires some additional consideration. In the crystal structure of albite, A1 is the only oxygen position that possesses two nearest Na atoms, the two Al–Na distances being 2.537 and 2.671 Å (Harlow and Brown, 1980) at 300 K. The difference of 0.134 Å between the two distances is rather great for an

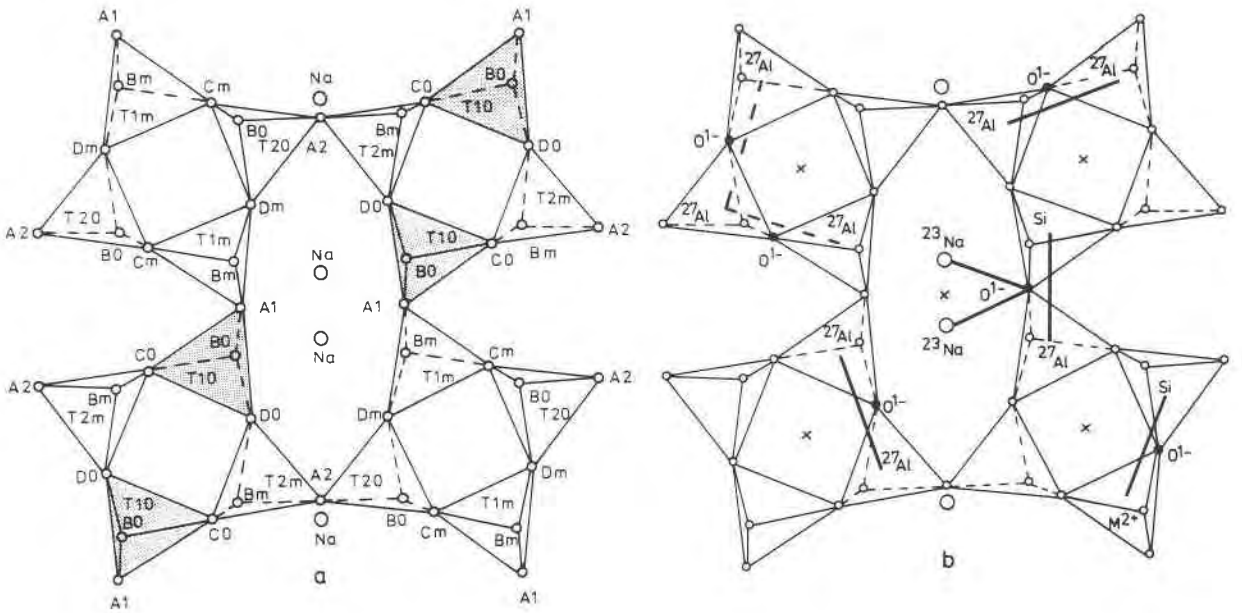

Fig. 7. Projection of the crystal structure of albite on the (201) plane. The projections of (a) and (b) are identical. In (**a**), the atomic positions of Na, Al, Si, and O are labeled using the notation of Megaw (1956). The T1(O) tetrahedra of the regular Al position in ordered albite are shaded. In (**b**), the most probable assignments of the six O^{1-} centers are marked by heavy lines. These were obtained from the g_{zz} eigenvectors of the mean positions of the centers that are assumed to be about parallel to the direction of the line connecting the two effective T positions. The two intense $O^{1-}/2^{27}Al$ centers, 1 and 2, are assigned to $Al_{T1(O)}$–$O^{1-}_{C(O)}$–$Al_{T2(m)}$ and $Al_{T1(O)}$–$O^{1-}_{D(O)}$–$Al_{T2(m)}$ bridges, respectively. The two weak $O^{1-}/2^{27}Al$ centers, 3 and 4, are assigned to $Al_{T2(O)}$–$O^{1-}_{C(m)}$–$Al_{T1(m)}$ and $Al_{T2(O)}$–$O^{1-}_{D(m)}$–$Al_{T1(m)}$ bridges, respectively. The $O^{1-}/^{27}Al \times 2^{23}Na$ center is assigned to a $Si_{T1(O)}$–O^{1-}_{A1}–$Al_{T1(m)}$ bridge that possesses two adjacent quasi-equidistant Na atoms. The O^{1-}/[Si,M^{2+}] center may be assigned to O^{1-} at D(m), with a bivalent cation, e.g., Mg^{2+}, substituting for one of the Si atoms at the two adjacent T1(m) and T2(O) tetrahedra.

equivalent SHF interaction by both Na atoms. Winter et al. (1977), however, showed that the Na–Al distances apparently approach each other at increasingly low temperatures.

In albite, the two Na atoms are not symmetrically equivalent with respect to the Al position, but their corresponding *s*-electron densities appear to be the same, as indicated by the equidistance and intensity ratio near 1:2:3:4:3:2:1 of the seven-line splitting. The total *s*-electron density at the nucleus of Na may be estimated for a value of A_{Na} = 4.2 MHz to be s^2 = 0.004 e at both Na positions (Fig. 8). This value may be compared with that of the $O^{1-}/^{23}Na$ center, $A \approx 4.5$ MHz, described for microcline by Marfunin and Bershov (1970).

Our mean value of A = 25 MHz for the ^{27}Al SHFS splitting in albite is somewhat larger than the value of A = 20 MHz of the six-line spectrum of "sunstone" (plagioclase) determined by Speit and Lehmann (1982). The line width of the sextet is broader by about 2×10^{-4} T than that of the 11-line spectra in albite; it is about twice as broad as that of the lines of the $O^{1-}/^{27}Al$ sextet in microcline (Matyash et al., 1982) and in "sunstone" (Speit and Lehmann, 1982). This greater width may be interpreted by the ^{23}Na SHFS splitting that is unresolved for many crystallographic orientations with respect to **B** and/or by the superposition of the spectra of two a'_1 centers (cf. Fig. 2, upper spectrum, additional shoulders in the sextet).

Abraham et al. (1972) reported A_{iso} = 8.6 MHz for $O^{1-}/^{23}Na$ centers in MgO and A_{iso} = 6.8 MHz in SrO. The considerably smaller value for albite is explained by the substantially greater Na–O distance compared to the Mg–O and Sr–O distances in the oxides of Mg and Sr.

O^{1-}/[Si,M^{2+}] center

Comparison of the eigenvector of g_{zz} of this center with possible O^{2-}–Si directions yields the position D(m) as the most probable site. Thus, this O^{1-} center is expected to bridge T1(m) and T2(O) tetrahedra. A single EPR line near g = 2 was detected first by Marfunin and Bershov (1970) in amazonite microcline at room temperature. It was interpreted in terms of an "Si–O^{1-}–Si" center. The same center was also noticed by Speit and Lehmann (1982) in labradorite, oligoclase, and microcline and then labeled as Si–O^{1-} $\cdots$ X (X = Mg^{2+}, Be^{2+}, or Zn^{2+}). Since the single-line O^{1-} center is apparently not perturbed by SHF interaction with an adjacent nuclear moment, it is generally assumed that it occurs at oxygen positions that are not bridging to Al tetrahedra. According to Speit and Lehmann (1982), a charge less than 3+ is needed at one of the adjacent tetrahedral positions for O^{1-} stabilization at room temperature. Bivalent ions that possess abundant

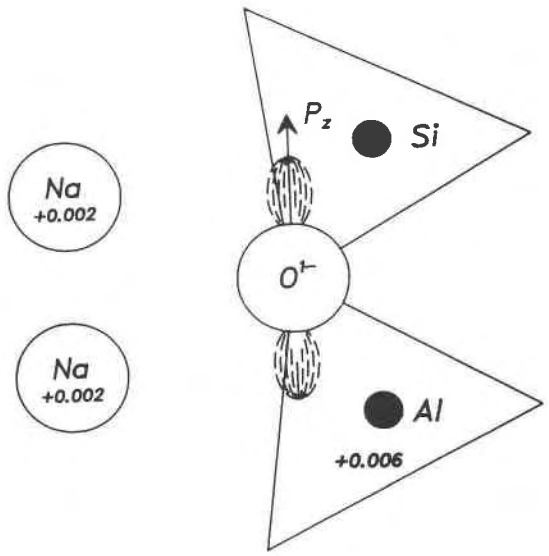

Fig. 8. Effective excess charges at adjacent Na and Al atoms estimated from the A values of the $O^{1-}/^{27}Al \times 2^{23}Na$. The **Z** axis, $\mathbf{P}_z$, of the $2p^5$ electron hole marks the effective direction of the SHF interaction; $\mathbf{P}_z$ is found to be approximately parallel to the T1(O)–T1(m) connecting line.

isotopes without nuclear moments are most likely for X (M in our notation), e.g., Mg^{2+} or a bivalent cation with small radius (Be^{2+}) at a T1(m) position.

The natural abundance (cf., e.g., Lozykowski et al., 1969) of ^9Be ($I = 3/2$) is 100%. However, its expected SHFS splitting is small. It is similar to that of ^{23}Na, i.e., too small to be resolved, the line width of the single line being $\Delta B_{pp} = 6 \pm 0.5 \times 10^{-4}$ T. For this reason, it is not possible to identify M = Be by use of conventional EPR. From a geochemical point of view, M = Mg^{2+} is most likely (e.g., Deer et al., 1963; Smith and Brown, 1988).

The $O^{1-}/[Si,M^{2+}]$ center without SHFS of adjacent ^{27}Al most probably can be created at the Dm, Cm, Bm, or A2 oxygen positions and is designated as h_m. The concentration of this center is at least 1×10^{-4} per formula unit.

In summary, it is concluded that the EPR spectra of O^{1-} give evidence for a large number of defects in basically well-ordered Amelia albite. All of the defects described in this paper are due to Al ions at Si positions or bivalent ions at Al or Si positions. In Amelia albite, 0.001–0.01 Na per formula unit are replaced by Ca (Winter et al., 1979; Harlow and Brown, 1980). Most feldspars contain traces of Fe, with Fe^{3+} substituting for Al^{3+} (Petrov et al., 1989) and Fe^{2+} substituting for Ca (Smith and Brown, 1988). Amelia albite contains 0.07% Fe_2O_3 (Sherriff and Hartman, 1985) and 1×10^{-4} to 2×10^{-4} Mn^{2+} per formula unit (Petrov et al., 1989). This substitution may be charge-compensated by excess Al (i.e., Al:Si > 1:3) at tetrahedral positions, bivalent cations at tetrahedral positions, and/or vacancies at the Na position.

Although vacancies at the Na position are certainly very likely, it has not been possible thus far to find direct evidence for them from the study of paramagnetic centers using EPR. The same applies for $(OH)^{1-}$ substitutions that are most likely to be present in Amelia albite. No SHFS due to protons could be discovered in our EPR spectra, however. No additional electron centers (e.g., SiO_3^{3-} or Ti^{3+}) complementary to the O^{1-} centers could be detected. These may be covered, however, by the four $O^{1-}/2^{27}Al$ centers in the region from $g \approx 1.9$ to $g \approx 2.1$ for different crystal orientations with respect to **B**, so that no single line due to an electron center can be observed.

Acknowledgment

We thank L. V. Bershov, IGEM of the Academy of Sciences, Moscow (USSR), for valuable discussion.

References cited

Abraham, M.M., Chen, Y., Kolopus, J.L., and Tohver, H.T. (1972) Radiation-induced $[Na]^0$ centers in MgO and SrO. Physical Review, 312, 4945–4951.

Barker, P.R. (1975) Hyperfine parameters of the Al center in smoky quartz. Journal of Physics, C8, L142–L144.

Deer, W.A., Howie, R.A., and Zussman, J. (1963) Rock-forming minerals, vol. 4, Framework silicates, p. 110. Longmans, Green & Co., Ltd., London.

Harlow, G.E., and Brown, G. (1980) Low albite: An X-ray and neutron diffraction study. American Mineralogist, 65, 986–995.

Hofmeister, A.M., and Rossman, G. (1985) A model for the irradiative coloration of smoky feldspar and the inhibiting influence of water. Physics and Chemistry of Minerals, 12, 324–332.

Ioffe, V.A., and Yanchevskaya, I.S. (1968) Electron paramagnetic resonance and thermoluminescence of irradiated single crystals of the aluminosilicates $NaAlSi_3O_8$ and $LiAlSiO_4$. Soviet Physics—Solid State, 10, 370–374.

Loewenstein, W. (1954) The distribution of aluminium in the tetrahedra of silicates and aluminates. American Mineralogist, 39, 92–96.

Lozykowski, H., Wilson, R.G.., and Holnj, F. (1969) EPR study of the hole centers in phenacite. Journal of Chemical Physics, 51, 2309–2321.

Marfunin, A.S. (1979) Spectroscopy, luminescence and radiation centers in minerals. Springer-Verlag, Berlin.

Marfunin, A.S., and Bershov, L.V. (1970) Paramagnetische Zentren in Feldspäten und ihre mögliche kristallchemische und petrologische Bedeutung. Doklady Akademii Nauk, USSR, 193, 412–414.

Maschmeyer D., Niemann, K., Hake, H., Lehmann, G., and Räuber, A. (1980) Two modified smoky quartz centers in natural citrine. Physics and Chemistry of Minerals, 6, 145–156.

Matyash, V.I., Bagmut, N.N., Litovchenko, C.A., and Proshko, Ya.V. (1981) Anwendung der EPR-Daten von Fe^{3+} zur Bestimmung von Strukturbesonderheiten der Alkalifeldspäte. Mineralogicheskii Zhurnal, 3, 76–80.

——(1982) Electron paramagnetic resonance study of new paramagnetic centers in microcline-perthites from pegmatites. Physics and Chemistry of Minerals, 8, 149–152.

Matyash, I.V., Brik, A.B., Zayac, A.P., and Masykin, V.V. (1987) Radiospektroskopie von Quarz. Naukova Dumka, p. 23, Kiew.

Megaw, H.D. (1956) Notation for feldspar structures. Acta Crystallographica, 9, 56–60.

Morton, J.R., and Preston, K.F. (1978) Atomic parameters for paramagnetic resonance data. Journal of Magnetic Resonance, 30, 577–582.

Nuttal, R.H.D., and Weil, J.A. (1981) The magnetic properties of the oxygen-hole aluminium centers in crystalline SiO_2. I. $[AlO_4]^0$. Canadian Journal of Physics, 59, 1696–1707.

O'Brien, M.C. (1955) The structure of the color centers in smoky quartz. Proceedings of the Royal Society of London, A231, 404–415.

Petrov, I. (1983) Correlation of EPR and optical absorption spectra of natural topaz. Fortschritte der Mineralogie, 61, 171–172.

Petrov, I., Yude, F., Bershov, L.V., Hafner, S.S., and Kroll, H. (1989)

Order-disorder of Fe^{3+} ions over the tetrahedral positions in albite. American Mineralogist, 74, 604–609.

Schnadt, R., and Räuber, A. (1971) Motional effects in trapped-hole center in smoky quartz. Solid State Communications, 9, 159–161.

Schnadt, R., and Schneider, J. (1970) The electronic structure of the trapped-hole center in smoky quartz. Physik der kondensierten Materie, 11, 19–42.

Sherriff, B.L., and Hartman, J.S. (1985) Solid-state high-resolution ^{29}Si NMR of feldspars: Al-Si disorder and the effects of paramagnetic centres. Canadian Mineralogist, 23, 205–212.

Smith, J.V., and Brown, W.L. (1988) Feldspar minerals. I. Crystal structures, physical, chemical and microtextural properties. Springer-Verlag, New York.

Speit, B., and Lehmann, G. (1982) Radiation defects in feldspars. Physics and Chemistry of Minerals, 8, 77–82.

Wertz, J.E., and Bolton, J.R. (1972) Electron spin resonance. Elementary theory and practical applications. McGraw-Hill, New York.

Winter, J.K., Ghose, S., and Okamura, F.P. (1977) A high-temperature study of the thermal expansion and the anisotropy of the sodium atom in low albite. American Mineralogist, 61, 921–931.

Winter, J.K., Okamura, F.P., and Ghose, S. (1979) A high-temperature structural study of high albite, monalbite, and the analbite-monalbite phase transition. American Mineralogist, 64, 409–423.

Manuscript received January 20, 1989
Manuscript accepted May 8, 1989